2012
International Symposium on Power Electronics,
Electrical Drives, Automation and Motion

PM Synchronous Motors for Automotive applications: Virtual Prototype and Experimental Testing

Romain-Bernard MIGNOT[*,**], Frédéric DUBAS[**], Christophe ESPANET[**], Fouad Charih[**]
and Didier CHAMAGNE[**]

[*] Phenix-International, Route de Noiron, F-70100 Gray
[**] ENERGY Department, UMR 6174 CNRS, FEMTO-ST Institute, University of Franche-Comte (UFC),
Parc Technologique, 2 avenue Jean Moulin, F-90010 Belfort

ABSTRACT – This study focuses on the design of a permanent magnet (PM) actuator for automotive. The analysis of the specification imposes the need for a powerful motor in a small volume. Following this, a first finite-element model (FEM) of the motor was developed using a methodology defined by the authors. A second numerical model was also developed using the MATLAB software. It represents a "virtual prototype" that enables to simulate, for different driving cycles and for different applications, the drive (motor+inverter) coupled to a mechanical load. This model takes into account the motor control too. The FE model has been validated by the realization and the tests of real a prototype.

KEYWORDS – Automotive, design, numerical, virtual prototype.

I. INTRODUCTION

The development of automotive passenger comfort is an important business in constant evolution. Past ten years, car manufacturers focused on the development of PM synchronous motors (PMSM). Indeed, a new need for quieter motors, involving both durability and electromagnetic compliance standards is required. A system that integrates a brushless motor and its associated control electronics become more interesting than a traditional DC motor.

In the first part, the paper describes how was calculated and designed the PMSM, using a FEM (developed with Flux2D software) and a methodology defined by the authors **[1-4]**. The numerical dynamic model (realized with MATLAB/SIMULINK software) of the geared motor is developed in the second part. The numerical results of the "virtual prototype" are compared with practical results obtained with a "real prototype".

II. SPECIFICATIONS

The project is to design a generic motor that can be placed at various strategic locations in a car. After a global study achieved by the industrial partner of the project, the main requirements are summarized in the following specifications:

- Voltage battery: 13.5 V;
- Rated/maximum Torque for rated speed: 0.22 Nm/0.44 Nm;
- Rated speed: 4100 rpm;
- Overall dimensions of the motor active parts: diameter lower than 60 mm and thickness lower than 10 mm.

III. MODELING OF ENGINE

A. Prototype Geometric and Physical Description

Flux2D software enables to model only an elementary section of the machine. The mesh of the geometry must be fine enough in the air-gap to obtain a correct precision. But the mesh should not be too dense in order to avoid long calculations. To automate the mesh, the authors have chosen a mesh length L_{mesh} constant in all machine and equal to the value of the air-gap $L_{mesh}=L_{air\text{-}gap}$. At the level of the air-gap, the mesh is $L_{mesh}=L_{air\text{-}gap}/2$.

This mesh is not optimal but has the advantage to lead to accurate results without manual intervention of the designer. The non-linear characteristics were used for stator laminations and rotor yoke to take into account magnetic saturation of materials.

B. Simulations Description

The aim of no-load simulations is to obtain for example the flux densities in the main points of the PMSM (i.e., the air-gap, the rotor teeth, and the stator yoke), the magnetic flux per pole, the back-EMF, the detent torque and the iron losses. The load simulations enable to obtain the electromagnetic torque and its ripples.

Figs. 1~2 show two results of no-load simulations (i.e., the flux density distribution and the back-EMF) and the Fig. 3 presents both statics and dynamic torques for a given load.

B1. Flux Density Distribution

Fig. 1 presents the flux density color shaded and the calculation points. This figure shows the local saturation of the stator yoke and teeth. The authors have deliberately chosen a rotor position where nearly the complete flux of one pole flows through a single tooth, leading to a strong saturation of the corresponding tooth.

978-1-4673-1301-8/12/$31.00 ©2012 IEEE

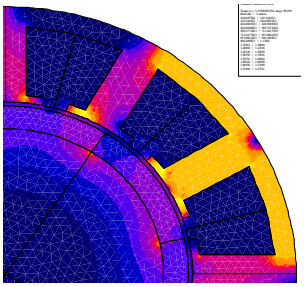

Fig. 1. The flux density in the PMSM.

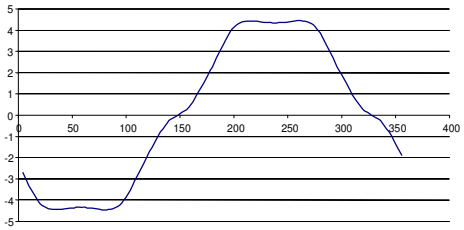

Fig 2. The back-EMF at 4100 rpm.

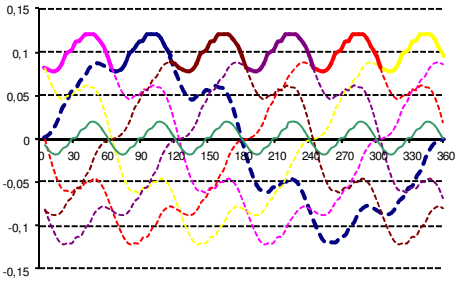

Fig 3. Static and dynamic torques obtained on ¼ stator yoke.

B2. Back-EMF

Fig. 2 presents the back-EMF waveform, which is trapezoidal with a maximum value of 4.5 V. The waveform is linked to the harmonics that come from the winding type and the rotor ring magnetization type. The slight ripples that appear on each back-EMF plate (positive or negative) are due to the teeth effects.

B3. Electromagnetic Torque

After a multi-position magnetostatic simulation, the static electromagnetic torque is obtained. By simple shift π/3p, the five other statics torques are deduced. The six static torques correspond to the six fed sequences. Assuming that the commutation angle is the natural angle of intersection between two consecutive static torques, we can deduce the dynamic torque and its average value.

C. No-load and On-load Simulations Conclusions

The FEM have validated the feasibility of developing a PM Brushless motor with a plasto-NdFeB ring. The constraints imposed by the specifications are feasible. In particular, the authors were able to plot the color shade of flux density, the flux lines in the PMSM, the detent torque and analyzed its impact on the electromagnetic torque in static and dynamic operations.

IV. VIRTUAL PROTOTYPE, EXPERIMENTAL VALIDATION AND ANALYSIS

A transient numerical model developed with MATLAB enables to not achieve control and to simulate the complete drive [see Figs. 4~5], including not only the motor and the inverter but also the mechanical load. Then, real driving cycle can be simulated.

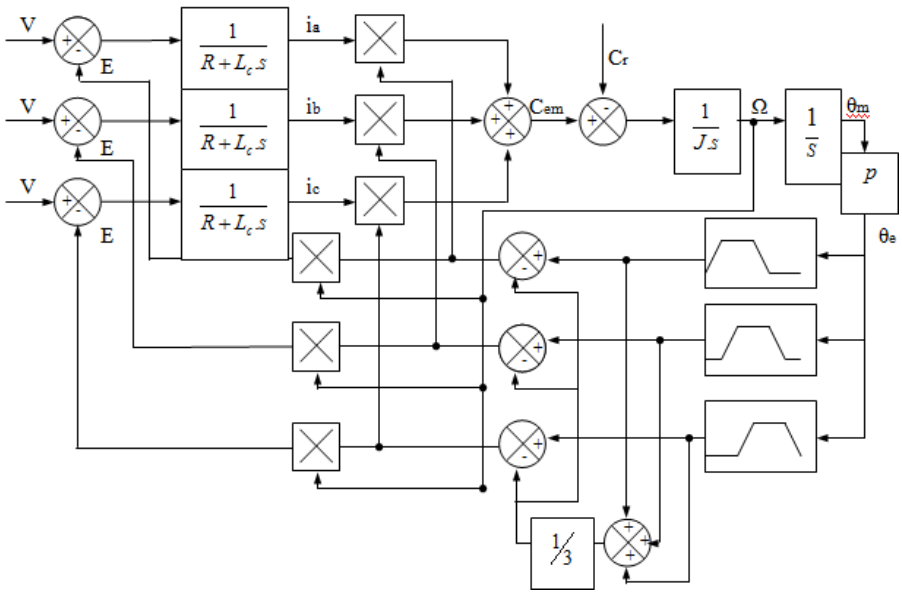

Fig 4. Diagram of the only PMSM.

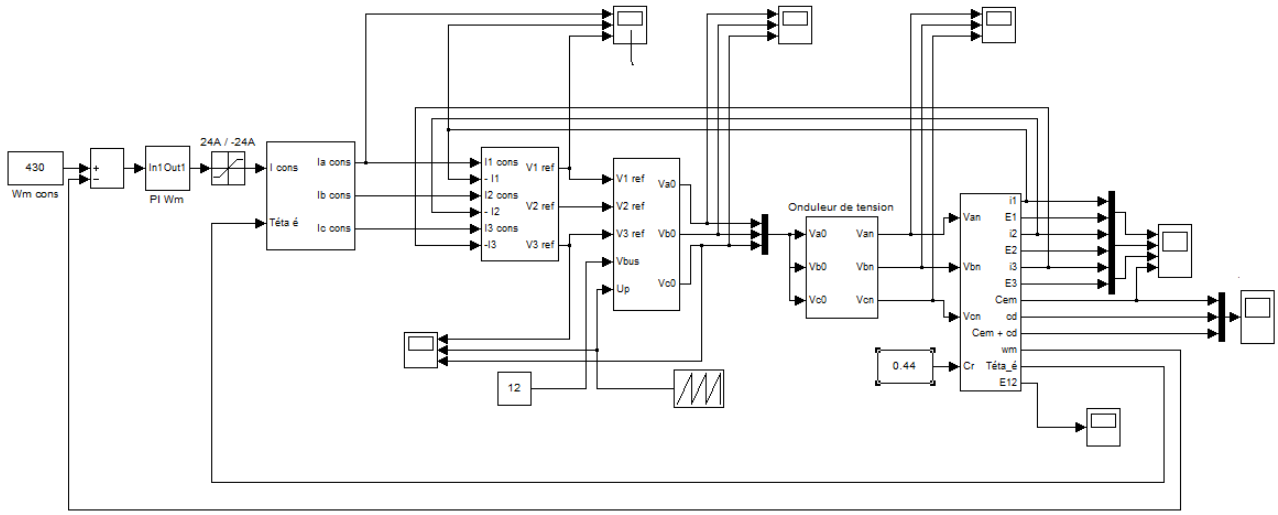

Fig 5. Complete diagram of the PMSM: the currents and speed of the motor are controlled.

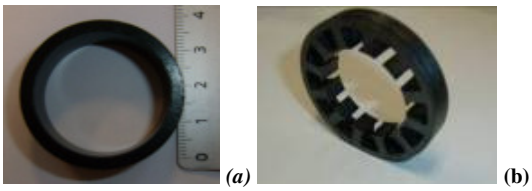

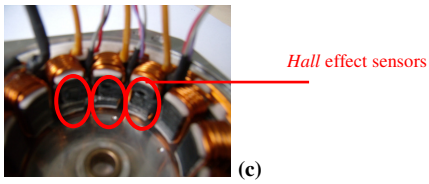

Fig 7. **(a)** PM ring; **(b)** Stator laminations; **(c)** Stator winding.

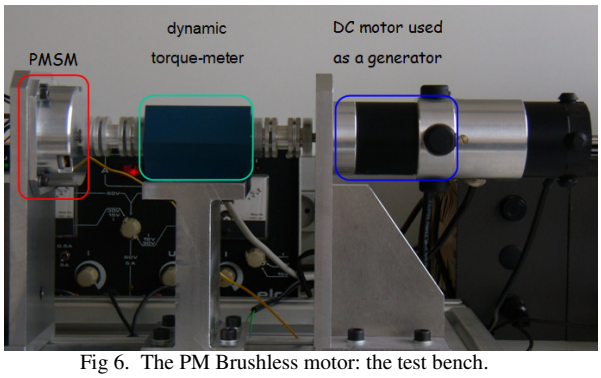

Fig 6. The PM Brushless motor: the test bench.

A. *Numerical Model of the Motovariator*

The numerical model of the PMSM [5] is based on the phase voltage and current equations, the electromagnetic torque and the second Newton law.

The numerical model of the inverter [6] is obtained assuming that the motor has three identical windings, which requires that the sum of the voltages is zero. The inverter is controlled with PWM and using a PI regulator in order to provide desired currents and thus to control torque [7-8].

B. *Prototype Description*

The test bench is represented in Fig. 6. It is composed of the PM Brushless motor prototype, a dynamic torque-meter and a DC motor used as a generator or a motor depending on the test type.

Fig. 7(a) shows the PM ring consisting of 8 poles. Fig. 7(b) shows the stator laminations consisting of 20 sheets (type: M600-50A). The stator uses concentric winding with 3 teeth per poles pair. Fig. 7(c) shows the Hall effect sensors that are located in a tooth in the middle of one coil. This enables the self-commutation of the PMSM.

Table I. Resistance and inductance of the stator winding.

	$R_l\ [\Omega]$	$L_p\ [\mu H]$	$M\ [\mu H]$	$L_c\ [\mu H]$
FEM		21.56	9.84	11.72
Measure	0.03	18.73	5.93	12.8

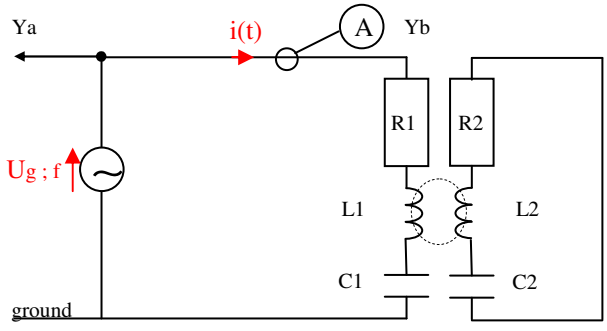

Fig 8: Inductance measurement of the coil n°1

C. *Validation of Numerical Results and Analysis*

1) Behn-Eschenburg Model

The Table I summarizes the values of the resistance and the inductance determined from both FEM and experimental tests, showing a good agreement.

Fig. 8 represents the inductance measurement of the coil n°1. The resistance value of the motor windings (i.e., R1 and R2) is determined by using the volt-ampermeter method. The values of the inductances (i.e., L1 and L2) and of the mutual (i.e., M1 or M2) of the motor windings are determined by measuring the resonant frequency of the forced oscillation circuit. This method requires the use of a capacitor (i.e., C1 and C2), whose capacity is known, and, in serial with the winding to indentify. A resistor could be eventually added in the circuit in order to limit the current at the resonant frequency.

2) Comparaison FEM/Virtual prototype/Experimental

Figs 9~10 compare the results of single and compound no-load back-EMF provided by the numerical model and the FEM. The results provided by the virtual prototype are validated.

Fig. 11 shows the result of the phase voltage obtained in practice. Analysis of the results shows that the actual waveform of the back-EMF is trapezoidal. The plate of the back-EMF is 5V. This value confirms the number of coils per phase. The value and direction of the magnetic flux density of the PM ring are validated.

Fig 12 shows the perfect difference of phase between the 120° current and the back-EMF in the phase 1. The virtual autopilot operates.

Fig 13 shows the modulation voltage of each phase.

Fig 14 focuses on the current flow for the value of I = 0A to 23A. This value is not instantaneous.

D. Conclusion on the Virtual Prototype and Analysis

A comprehensive numerical model in MATLAB of the PMSM, coupled with its control electronics and power, has been developed. This virtual prototype has been adapted and adjusted with precision through to the results provided by the FEM previously developed.

V. CONCLUSION

In this paper, the authors present a methodology for the selection and the design of a PM Brushless motor for automotive applications. Experimental results have validated the numerical model results. The proposed tools can be used in the future for other designs without prototype construction. The industrial objective of saving time, reducing investment and financial costs can be therefore achieved more easily.

REFERENCES

[1] F. Wurtz, "**A new approach to the design stress of electric machine**", Doctoral thesis, INPG, (1996)

[2] M. Almaki, "**Implementation of a software design support and optimization of electric actuator**", JCGE, Cachan, (1998)

[3] F. Wurtz, et C. Espanet, J.Bigeon "**Methodological guidelines for the use of analytical and numerical models and the design process of an electromagnetic device**", IEEE trans. of mag. Vol. 34, N°5, (1998).

[4] F. Badin, "**Need for an assessment tool overall cost**", INREST. Lyon, (1998).

[5] Z. Wu, D. Depernet, C. Kieffer, F. Dubas, D. Hissel, C. Espanet – "**Electrical motors design for hybrid heavy-duty electrical power train**", Vehicle Power and Propulsion Conference, 7-10 Sept. 2009, pp 486 -493

[6] M.PINARD, "**Converters and power electronics, control / description / implementation**", éditions Dunod, Paris 2007

[7] A.CUNIERE et G.FELD, "**Examples of simulation in SIMULINK**", ENSC 2007

[8] SITELEC, "**Synchronous machines, technologies and modes of supply of synchronous machines**", http://sitelec.free.fr/cours/msyn.pdf

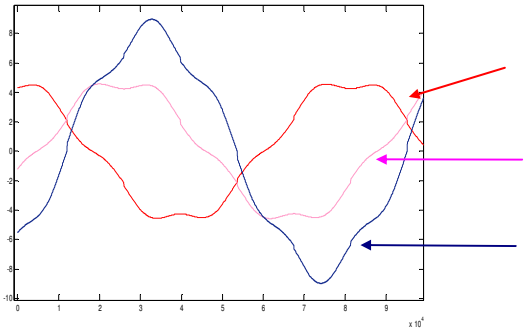

Fig 9. Results obtained with the "virtual prototyping" (4100 rpm).

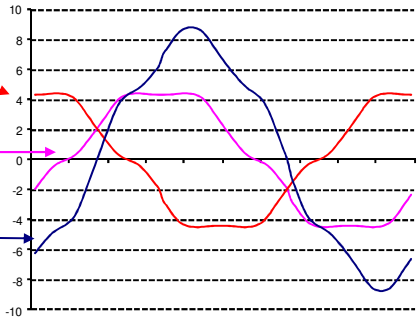

Fig 10. Results obtained with the back-EMF (4100 rpm).

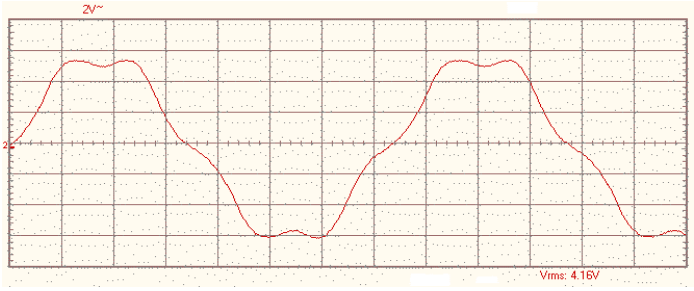

Fig 11. The back-EMF in a coil provided by experimental tests (4100 rpm).

(2V per tile horizontally and 0,5ms per tile vertically)

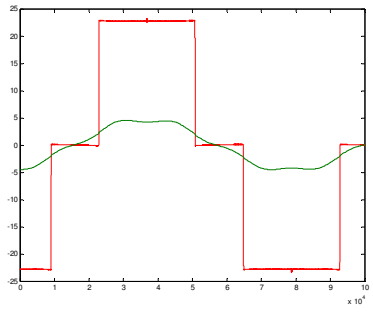

Fig 12: Current and voltage in the coil n°1.

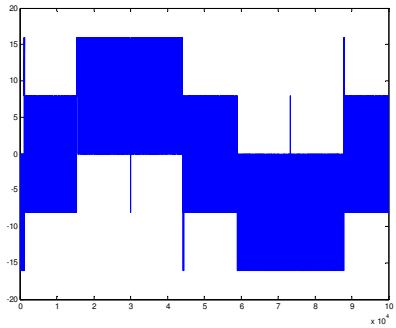

Fig 13: Power supply voltage modulated (coil n°1).

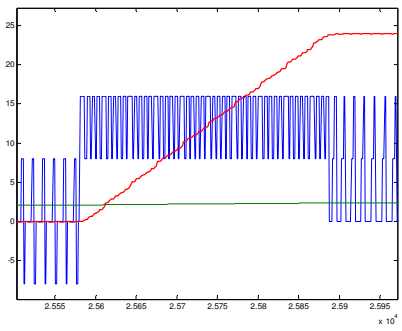

Fig 14: Focuses on the current and on the supply voltage modulated (4100 rpm).